International Journal of Precision Engineering and Manufacturing
https://doi.org/10.1007/s12541-019-00187-w

Online ISSN 2005-4602
Print ISSN 2234-7593

REVIEW PAPER

Robotic Machining: A Review of Recent Progress

Seong Hyeon Kim[1] · Eunseok Nam[2] · Tae In Ha[1] · Soon-Hong Hwang[1] · Jae Ho Lee[1] · Soo-Hyun Park[1,3] · Byung-Kwon Min[1]

Received: 29 November 2018 / Revised: 6 June 2019 / Accepted: 24 June 2019
© Korean Society for Precision Engineering 2019

Abstract
The use of industrial robots is widespread in diverse manufacturing fields. Hence, there have been attempts to use robot for machining processes instead of machine tools. However, limited machining accuracy has been a major obstacle hampering the adoption of robotic machining systems. Recently, substantial research has been carried out to address this issue. In this paper, recent progress in robotic machining has been summarized, such as kinematic calibration and compliance error compensation to improve the accuracy of robotic machining. Auxiliary units for improving the performance of robotic machining systems are also discussed.

Keywords Manufacturing system · Robot manipulator · Industrial robot

1 Introduction

Industrial robots have been used for various applications in production systems because they have many advantages, such as large workspaces, high degree of freedom (DOF), flexibility, and cost-effectiveness [1–3]. Compared to dedicated machine tools, industrial robots have large workspaces that can easily be extended by the addition of stages or mobile platforms. Robotic machining can be highly flexible because robots can be adjusted for a variety of machining processes by changing the end-effectors or tools attached to the manipulator. As robotic machining systems have more DOF than machine tools, more complex parts can be machined. Robots can also form workcells with other robots or machine tools. Therefore, the use of robots is increasing as the manufacturing paradigm shifts from mass production to mass customization. Furthermore, the total costs of robotic machining systems are less than those of dedicated machine tools. However, despite the advantages, the implementation of robotic machining systems is still in its infancy due to their low machining accuracy. Although most industrial robots are used for welding and material handling processes, the adoption of robots for other machining processes has increased. Thus, substantial research has been carried out to analyze and reduce robotic machining errors and improve the performance of robotic machining systems.

In this paper, the application of robots to machining and methodologies for improving robotic machining accuracy are reviewed. Robotic machining systems and processes are summarized in Sect. 2. Algorithms to improving robotic machining accuracy and additional hardware setup for robotic machining systems are reviewed in Sects. 3 and 4, respectively. Section 5 concludes the review.

✉ Byung-Kwon Min
bkmin@yonsei.ac.kr

Seong Hyeon Kim
shkim88@yonsei.ac.kr

Eunseok Nam
esnam86@kitech.re.kr

Tae In Ha
gkxodls@yonsei.ac.kr

Soon-Hong Hwang
hwang.soonhong@yonsei.ac.kr

Jae Ho Lee
ljh9303@yonsei.ac.kr

Soo-Hyun Park
elga79@yonsei.ac.kr

[1] School of Mechanical Engineering, Yonsei University, 50 Yonsei-ro, Seodaemun-gu, Seoul 03722, Republic of Korea

[2] IT Converged Process R&D Group, KITECH, 143, Hanggaul-ro, Sangnok-gu, Ansan-si, Gyeonggi-do, 15588, Republic of Korea

[3] Global Technology Center, Samsung Electronics Co., Ltd., 129 Samsung-ro, Yoengtong-gu, Suwon-si, Gyeonggi-do 16677, Republic of Korea

Published online: 05 August 2019

2 Robotic Machining Systems and Processes

2.1 Robotic Machining Systems

A typical robotic machining system has a serial robot arm to exploit the large workspace and confer flexibility to the system. As shown in Fig. 1a, a robotic machining system consists of a serial manipulator and a spindle attached to the end-effector. Various configurations of robotic machining systems have been proposed to improve machining performance. For example, to increase the structural rigidity of robotic machining systems, instead of manipulating the DOF, a spindle can be attached to the fifth joint of the robot manipulator, as shown in Fig. 1b. This is because a six-axis structure is vulnerable to external forces and five DOF is sufficient for machining a three-dimensional (3-D) structure. The spindle can be attached to the end-effector in different ways, based on the required machining process. For milling or routing processes, the spindle is attached vertically, while for drilling processes, the spindle is connected to the end-effector in parallel to reduce the impact of the cutting force acting on joint five.

2.2 Machining Applications

Research on robotic machining systems can be categorized according to the machining load. To date, robotic machining systems have generally been applied to processes with small machining loads, such as polishing and grinding [4–17]. Typically, these processes remove small volumes and exert little abrasive force. As the main purpose of the polishing operation is not to change the shape of a structure but to make its surface finer, it is not necessary for the processes to maintain highly accurate position control. Therefore, robot manipulators have been used for these applications earlier than in other processes. As the positions and orientations of robot manipulators can easily be adjusted, they can always maintain tools normal to the machined surface. Thus, polishing and grinding using robots yield higher-quality surfaces than do three-axis machine tools [18]. The welding process has a small machining load, and is thus another application of robotic machining systems [19–22]. Except in the case of friction-stir welding, electrodes or laser sources are used for welding processes. As welding processes do not involve contact with the workpiece, position errors due to machining loads are almost negligible. Furthermore, the tool paths for welding are generally less complex than those used for milling or cutting processes. Thus, robotic machining systems have been widely used for welding processes. Figure 2 shows a welding system using a robot manipulator. The robot welding system is attached to a mobile vehicle to enlarge the workspace. Robotic machining systems have also been applied to the waterjet cutting process, as shown in Fig. 3 [23–25]. Like robotic welding processes, waterjet cutting is a non-contact process. Although the water pressure can lead to deviations in the positions of the robots, the position error is relatively small compared to that in contact machining processes.

In conventional applications, robotic machining systems have been used only for machining processes that do not involve large machining loads or require high path accuracy. Furthermore, the workpiece materials are usually relatively soft and light, and therefore do not induce large machining forces. For example, aluminum and plastic are representative

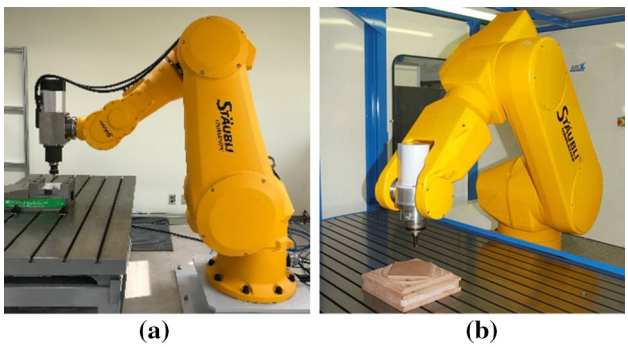

Fig. 1 Serial robotic machining systems; **a** spindle attached at the end-effector, **b** spindle attached to 5th joint

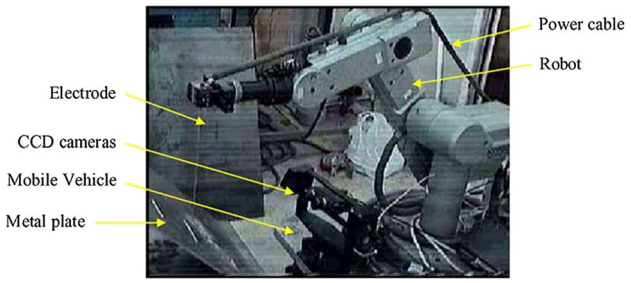

Fig. 2 Mobile robotic welding system [20]. (Adapted from Ref. [20] with permission)

Fig. 3 **a** Wet abrasive jet machining with industrial robot; **b** cutting edge handling parameters for the robot guidance [25]. (Adapted from Ref. [25] with permission)

Table 1 Materials used for robotic machining

Grinding/ polishing/ finishing	Aluminum [4], stainless steel 304L [6], and Inconel 718 [7]
Welding	Aluminum [22] and steel [21]
Waterjet	FRP [24], carbide [25], and rubber [23]
Drilling	Aluminum alloy [27, 28, 30] and titanium [32]
Milling	Aluminum [38, 39], plastics [34], and CFRP [35]

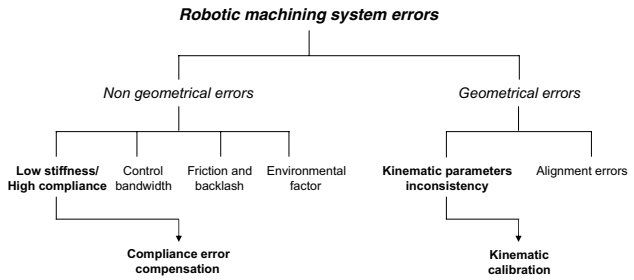

Fig. 4 Robotic machining system errors

materials for workpieces. Some of the materials that can be machined by robotic machining systems are summarized in Table 1. Recently, robotic machining has also been applied to drilling [26–33] and milling [34–41] processes that induce large machining forces and may involve advanced and hard-to-cut workpiece materials such as titanium and carbon fiber reinforced plastics (CFRP) for aerospace and automotive industries. Unlike welding and material-handling processes, which require only position repeatability, milling and drilling require high path accuracy. Therefore, many studies have been conducted to analyze and compensate robotic machining errors. The trends in research on robotic machining systems, towards improving machining accuracy and performance, will be introduced in the following sections.

3 Improving the Machining Accuracy of Robotic Machining Systems

There are two major sources of robot positioning errors, as shown in Fig. 4: geometrical errors and non-geometrical errors. Geometrical errors are caused by misalignment of the robot workcell and discrepancies between the nominal and actual values of kinematic parameters, such as the link length, assembled angle, etc. Geometrical errors do not affect the repeatability of a robot manipulator. However, as these kinematic parameters are used in robot controllers to generate reference trajectories and control the poses (position and orientation) of the robot end-effector in Cartesian space, discrepancies lead to deterioration in the path accuracy of the robot manipulators. These effects are important in robotic machining applications [42–47]. It has been reported that geometrical errors account for approximately 90% of position error when the external wrench (force/torque) applied to the robot end-effector is relatively small [43].

Non-geometrical errors are caused by low stiffness of the robot manipulator, environmental factors, limited bandwidth of the controller, and friction/backlash [48–50]. The wrench acting on the end-effector can deform the manipulator components, leading to compliance errors. In general, the stiffness of industrial robot manipulators is 50 times smaller than that of conventional computerized numerical control (CNC) machine tools [51]. Thus, considerable deflection can occur in the end-effector during the machining process due to the cutting force. Environmental factors, such as temperature, atmospheric pressure, and humidity affect the physical properties of manipulator components, causing undesirable motions [43]. As the moving mass of a robot manipulator is large and the control cycle time of an industrial robot controller is about 4–12 ms, the bandwidth of a robot controller is relatively low, leading to limitations in the tracking performance. Furthermore, friction and backlash can deteriorate the positioning accuracy of the robot manipulator [52]. Among these non-geometrical errors, substantial research has shown that compliance errors are the most significant. Although position repeatability and payloads are general requirements for robot manipulators when applied to non-machining processes, overall structural rigidity is of significant importance in robotic machining. Therefore, when constructing a robotic machining system, the stiffness of the robot manipulator should be considered in addition to position repeatability, path accuracy, and payload.

In this section, algorithms for improving the machining accuracy of robotic machining systems are reviewed. Among the many factors that affect accuracy, kinematic parameter discrepancies and compliance errors are the most influential.

3.1 Kinematic Calibration

Kinematic parameter discrepancies are inconsistencies in the kinematic parameters, such as incorrect link lengths, assembly tolerances, etc. Incorrect kinematic parameters degrade robot position and orientation accuracy. Therefore, studies have been carried out to identify and model kinematic parameters, and thus improve the accuracy of robots. Barker [53] proposed a kinematic error calibration algorithm based on Denavit–Hartenberg (D–H) parameters. The proposed method evaluates kinematic errors simply by measuring the end-effector position at different joint angles. However, the D–H parameter-based kinematic error model has a singularity problem, because small errors in the Z-axis of the two parallel axes have a significant effect on the remaining parameters. Hayati and Mirmirani [54]

proposed a new modeling method that adds a Y-axis rotation parameter between two parallel or nearly parallel axes and verified their proposed method by simulating a Stanford manipulator and a 6R serial robot. Ye et al. [55] developed an algorithm that identified kinematic parameters iteratively using a D–H parameter-based kinematic model. Using the proposed algorithm, the position of the base frame and kinematic parameters of a robot were identified simultaneously and calibration was applied to reduce the position error from 0.96 to 0.47 mm. Ha [56] proposed a new calibration method based on displacement of the end-effector in two configurations. The parameters were calibrated to eliminate the discrepancy between the measured and predicted displacement. This calibration method has the advantage of not requiring a transformation between the robot base frame and the measurement frame, because the displacement of the end-effector remains consistent regardless of the frame.

Screw-theory-based kinematic error models have also been studied to address the singularity problem of the D–H parameter-based model. Okamura and Park [57] proposed a kinematic calibration method based on a product of exponential (POE) formula. In their proposed method, the forward kinematics are expressed as follows:

$$\mathrm{f}\left(x_1,\ldots,x_n\right) = e^{A_1 x_1} e^{A_2 x_2} \ldots e^{A_n x_n} \mathrm{M} \tag{1}$$

where x, M, A_i are the joint variables, transformation matrix between the world frame and tool frame in the home position, and the matrix representing the transformation between the $(\mathrm{i}-1)$th and the ith frames, respectively. Unlike in the case of the D–H parameter-based model, the singularity problem does not occur even when two adjacent joints are parallel or nearly parallel because the $\mathrm{A_i}$ matrix varies smoothly with the joint axes. However, this model has the disadvantage of being dependent on many parameters, requiring six parameters per axis. Hence, Yang et al. [58] proposed a novel kinematic error model called the minimal POE. Four kinematic parameters are required per axis for the minimal POE model, which is less than that required by the conventional POE-based model. Because the number of parameters is decreased and each parameter is independent, computation time decreases and the algorithm converges better. In tests, the mean position error of the proposed model was 0.663 mm, compared to 0.876 mm using the traditional POE-based model. Wu et al. [59] proposed a minimal POE-based kinematic calibration algorithm based on end-effector position data. While the traditional model requires both position and orientation measurements for kinematic parameter identification, their proposed method can identify kinematic parameters based only on position measurements. The mean position error of the proposed model in tests was 0.266 mm, compared to 0.788 mm in the case of the traditional POE-based model. As orientation is calculated from position data in the traditional algorithm, small errors in that data can significantly affect orientation, leading to a deterioration in the accuracy of the calibration. Another reason for this deterioration is the method used to create the cost function. The traditional model constructs the cost function using two types of data (position/orientation) with different units. This process adds an undesired weighting, decreasing calibration accuracy.

To improve the accuracy of robots, modeling methods that evaluate both kinematic and non-kinematic parameters have been studied [60–62]. Jang et al. [62] proposed a new method to calibrate kinematic and non-kinematic errors simultaneously. In this method, joint compliance and gear transmission errors are considered the causes of non-kinematic errors. They established a D–H parameter-based error model that include both kinematic and non-kinematic errors, and Radial Basis Function Network (RBFN) was used to evaluate the parameters. The distance accuracy, defined as the (length of commanded path-measured path)/commanded path, improved from 0.920 to 0.154% when the proposed algorithm was applied. Nubiola and Bonev [63] established a D–H parameter-based error model that include kinematic errors, joint stiffness, and nonlinearity in joint six. In total, 29 parameters (19 kinematic parameters + 4 compliance parameters + 6 parameters related to joint six) were determined using the linear least square method. Figure 5 shows the experimental setup used to identify kinematic errors. A laser tracker and eight spherically mounted reflectors (SMRs) were used to measure the position of the robot end-effector precisely. The calibration decreased the mean position error from 0.986 to 0.363 mm.

3.2 Compliance Error Compensation

Industrial robot manipulators are composed of revolute joints that are connected in series. This structure has merits for large workspaces but is ultimately disadvantageous in its

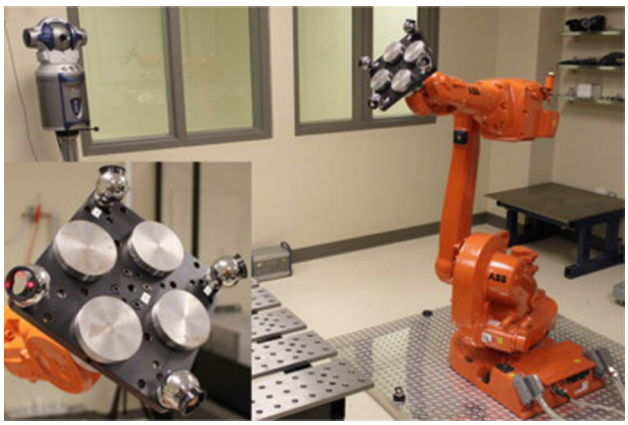

Fig. 5 Experimental setup with the 6R serial robot and laser tracker [63]. (Adapted from Ref. [63] with permission)

low stiffness, which leads to structural deformation by external forces. During the machining process, cutting forces acting on the end-effector of the manipulator can cause deflection. Compliance errors constitute a significant proportion of the robotic machining error. However, because deformation of manipulator structures is not measured by the encoder, which is attached to the motor, a standard robot controller cannot compensate the compliance errors. Therefore, a substantial amount of research has focused on modeling the stiffness of the manipulator and compensating the compliance errors.

3.2.1 Stiffness Model and Identification Method

Stiffness-modeling methods can be categorized into two types: the virtual joint method (VJM), which describes elastic components as lumped-parameters [63–68]; and finite element analysis (FEA), which is used to calculate elastic deformation according to Euler–Bernoulli theory or by using volumetric FE computer-aided design (CAD) tools [69–74]. A major advantage of FEA is its accuracy, but it requires high computational expense and advanced modeling skills. On the other hand, it is easy to derive stiffness models using VJM, but they are less accurate than those developed using FEA. In general, VJM has been widely applied to robotic machining applications due to its computational efficiency and acceptable accuracy.

The conventional stiffness matrix model was proposed by Salisbury [64], in which the transmission parts (gearbox, actuator, etc.) of the joints are considered as the main sources of compliance errors. A virtual torsional spring is used to represent the stiffness of each joint and the conventional stiffness model is derived as follows [75]

$$K_X = J^{-T} K_q J^{-1} \tag{2}$$

where K_X, $K_q = diag\left[K_{\theta 1}, K_{\theta 2}, \ldots, K_{\theta 6}\right]$, and J represent the Cartesian stiffness matrix; the joint stiffness matrix; and Jacobian matrix, which describes the relationship between the Cartesian and joint coordinates, respectively. However, the conventional stiffness matrix model is valid only when no load is applied to the robot manipulator. Thus, conservative congruence transformation (CCT) was proposed by Chen et al. [76, 77]. CCT describes the relationship between Cartesian and joint stiffness matrices by taking into account the variation in manipulator geometry caused by applied loads, and is derived as [78]

$$K_X = J^{-T}\left(K_q - K_C\right)J^{-1} \tag{3}$$

where $K_c = \left[\frac{\partial J}{\partial \theta_1}, \ldots, \frac{\partial J}{\partial \theta_6}\right]^T w$ is the complementary stiffness matrix and $w = \left[F_x, F_y, F_z, T_x, T_y, T_z\right]^T$ represents a wrench containing six DOF forces and moments. Unlike previous studies, which considered a link to be perfectly rigid, Yoshikawa et al. proposed modeling for a flexible link, which they modeled as several virtual rigid links with passive joints [66, 79]. Abele et al. [80] proposed an enhanced compliance model that includes link deformation as well as elasticity in the transmission parts (gears and bearings). To describe compliance effects more accurately, each joint is modeled as a virtual spring with three DOF. Furthermore, Schneider et al. [81] proposed a more complicated stiffness model, in which each joint stiffness consists of six DOF virtual springs, meaning that the stiffness model had a total of 36 DOF. Marie et al. proposed a fuzzy logic model to represent nonlinear stiffness, which is not taken into account by parametric models. The proposed fuzzy logic model has been shown experimentally to have advantages in terms of simplicity, rapidity and robustness [82].

Two approaches can be used to identify the stiffness of a manipulator experimentally: local and global. The local identification method is used to measure the elasticity of each axis separately; a force is exerted on one axis and its deflection is measured [41, 80, 81, 83, 84]. This process is carried out sequentially along the serial link. The force must be exerted entirely on the target link, without affecting the other links, which therefore must be clamped. As the stiffness of each joint is calculated separately, the stiffness of a given joint can be identified without compliance effects from the other joints or link deformation. A typical experimental setup for local evaluation is shown in Fig. 6. In the global identification method, a force is exerted on the end-effector of the manipulator and the deflection of the end-effector is measured simultaneously [78, 85–87]. The merits of the global method are ease of installation compared to the local method. However, as the deflection and Cartesian

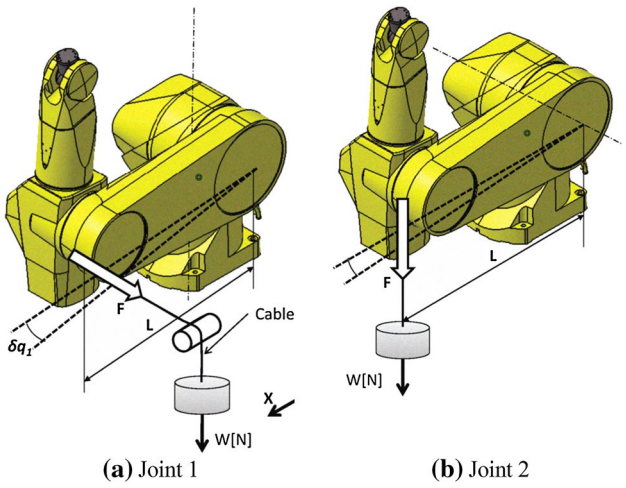

(a) Joint 1 **(b)** Joint 2

Fig. 6 Schematic of experimental setup for stiffness identification (local identification method) [84]. (Adapted from Ref. [84] with permission)

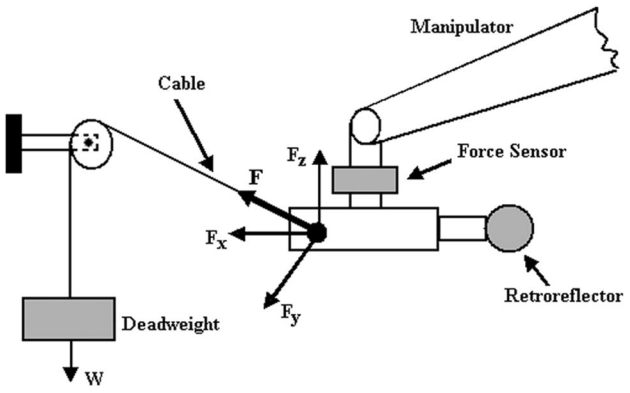

Fig. 7 Schematic of experimental setup for stiffness identification (global identification method) [78]. (Adapted from Ref. [78] with permission)

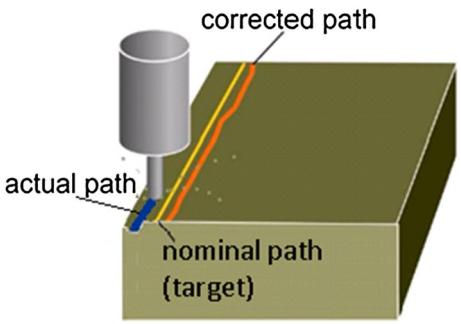

Fig. 8 Schematic of offline tool path compensation for compliance error [94]. (Adapted from Ref. [94] with permission)

stiffness are dependent on the manipulator configuration, many experiments are required with various configurations before the value of the stiffness converges. The experimental setup for the global method is shown in Fig. 7.

3.2.2 Tool Path Modification

Most commercial robot controllers have closed architectures, which make it difficult to implement control algorithms. Thus, compensation algorithms have been proposed, which apply offline modifications to the target trajectory based on the estimated tool deflection, as shown in Fig. 8 [84, 87–92]. Slavkovic et al. [87] proposed offline path correction to compensate the errors induced by cutting forces. Using the conventional stiffness model and a mechanistic cutting force model, machining errors were predicted, and part program was then modified to compensate the estimated errors. A machining experiment was conducted on an aluminum workpiece, and the machining error decreased to $< \pm 100$ μm. Klimchik et al. proposed a compliance compensation method that considers both a nonlinear stiffness model and a dynamic model of the robotic machining process. Unlike earlier research, which took only static interactions between the tool and workpiece into account, their dynamic behavior was studied. This can improve machining accuracy and avoid chattering effects [88]. Cordes and Hintze [92] proposed a compliance and hysteresis model to describe reversal error at zero crossing. Reversal error arises in joints due to the sudden change in the sign of frictional torque at zero velocity. An aluminum milling circle experiment showed that the proposed method improved roundness by 31%. Abele et al. [93] proposed an offline tool path adaptation method for milling. Using a camera, the workpiece machined by the robot is captured and restored in a digital format using a Dexel model. The Dexel model is compared to the desired shape. The path offset is calculated based on the results of this comparison and an adjusted tool path is generated. Then, the workpiece is machined using the modified tool path. The results of the experiment demonstrated that a tolerance of 0.21 mm could be achieved.

Online compensation has also been proposed, with the help of robot manufacturers or special functions in robot software. However, because control structure modifications are unavailable, compensation algorithms are restricted to tool-path correction based on estimated errors [39, 51, 82, 95–99]. Pan and Zhang [39] proposed a real-time compensation algorithm for machining errors caused by low stiffness. The conventional stiffness model was adopted rather than the CCT, because it is easy to implement and the complementary term in the CCT can be neglected in this application. Using the stiffness model and force measured by a six DOF force/torque sensor attached at the end-effector, the tool deflection for each cycle was predicted; the target position was then modified according to the estimated error. In an aluminum block machining test, the machining error decreased from 0.4 to < 0.1 mm. Zaeh and Roesch [98] proposed a model-based fuzzy controller that compensates machining errors and avoids vibrations. In that study, preliminary cutting experiments were carried out to measure cutting-force-induced deflections for various tool paths. A real-time compensation algorithm was implemented based on the stiffness model and a force/torque sensor. Different control strategies were adopted depending on the machining states (stable or chatter). A schematic diagram of the control algorithm is shown in Fig. 9.

3.2.3 Posture Optimization

Posture optimization methods have been proposed to reduce compliance errors. A performance index has been suggested to evaluate the structural rigidity of the manipulator according to the cutting force. The performance index is used to identify a rigid posture that reduces compliance errors.

Guo et al. [100] proposed a performance index to optimize the manipulator posture for drilling processes. Under

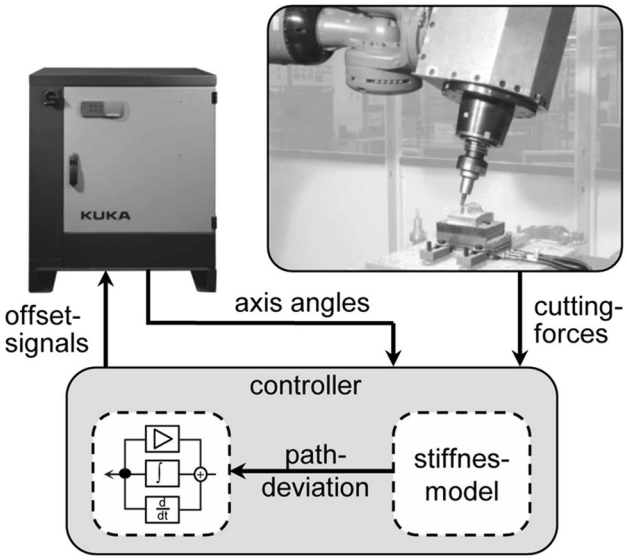

Fig. 9 Structure of real-time tool path deviation method for compliance error compensation [98]. (Adapted from Ref. [98] with permission)

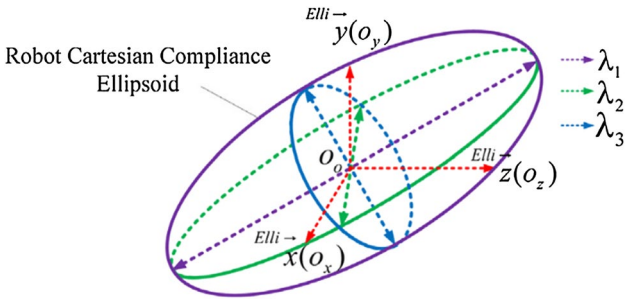

Fig. 10 Cartesian compliance ellipsoid [101]. (Adapted from Ref. [101] with permission)

the assumptions that orientation deformation of the end-effector is negligible compared to translational deformation, and that cutting torque has little effect on translational deformation, the relationship between translational deformations and external forces can be expressed as:

$$\Delta X_t = C_{tt} F \tag{4}$$

where C_{tt} is the translational compliance matrix, $\Delta X_t = \left[\Delta x \ \Delta y \ \Delta z\right]^T$ is the translational displacement of the end-effector, and $F = \left[F_x \ F_y \ F_z\right]^T$ is the force applied to the end-effector. Using (4), a Cartesian compliance ellipsoid was suggested, and the performance index was defined as the volume of the ellipsoid with respect to the exerted force at a given configuration, as shown in Fig. 10. Because the overall compliance of the manipulator is proportional to the index, i.e., the volume of the ellipsoid, the posture of the manipulator should be selected such that the index is minimized. To verify the proposed method, a drilling experiment was carried out at the initial and optimized postures. The experimental results showed that the translational error of the end-effector decreased about 25%.

Bu et al. [101] proposed two performance indices that consider the stiffness in the drilling and lateral directions. This is because, although the thrust force is dominant in the drilling process, deformations can also occur in directions other than that of the applied force due to the structural characteristics of the robot. The proposed indices take into account the stiffness of the robot with respect to the direction of the force; thus, the structural rigidity of the manipulator in a specific direction can be maximized. To evaluate the effectiveness of the indices, drilling experiments were carried out using the initial and optimized postures; the displacement error in the drilling direction decreased about 40%.

Lin et al. [102] presented an index based on the force model of drilling. It is assumed that the direction of the force was the same as the axial direction of the spindle. The contribution of this optimization method was evaluation of the stiffness in the entire workspace rather than in the local workspace. A stiffness map was presented to evaluate the stiffness of the workspace using the index. Experiments and simulations were carried out to verify the performance of the index.

To date, various performance indices have been proposed to evaluate the structural rigidity of the manipulator and perform posture optimization. However, because most studies have performed posture optimization for only the initial point rather than the entire tool path, the proposed methods can be applied only to drilling process as a result. Therefore, studies on performance indices that take into account the stiffness of the entire tool path are required to reduce the errors associated with various machining process, such as milling, routing, etc.

4 Auxiliary Units for Improving Machining Performance

Approaches that utilize external devices have been proposed to reduce the effects of the low stiffness and low bandwidth of robot manipulators and maximize the workspace. In this section, external devices such as electromechanical compensation mechanisms, external measurement systems, and mobile platforms are introduced.

4.1 Additional Actuation System

One of the most notable progresses in robotic machining systems was developed by the COMET consortium [103]. The robotic machining system proposed by COMET included a piezo-actuated high-dynamic compensation mechanism

(HDCM) for fast and accurate positioning of the spindle. HDCM was used to compensate path deviations detected by an external optical measurement system and high frequency errors that exceed the bandwidth of the robot.

Puzik et al. [105] designed a serial compensation mechanism based on piezo actuators and flexure systems. Schneider et al. [106] proposed a parallel mechanism for improving the stability of a system by increasing the lowest natural frequency such that it is higher than that of the robot. Olofsson et al. [107] identified the dynamic properties of an HDCM system and designed a model-based feedback control system. Sörnmo et al. [104] carried out a milling experiment using a robotic machining system with HDCM, as shown in Fig. 11. Path deviation was detected by comparing the differences between the position of the end-effector measured by an optical tracking system and that specified by the robot controller. The path deviation was input to the HDCM controller for reference. The results of the milling experiment demonstrated that the HDCM system enhanced the machining quality significantly compared to the uncompensated system, reducing the maximum machining error from 67 to 24.5 μm and the standard deviation of the surface profile from 14.9 to 4.7 μm.

4.2 External Measurement Systems

Measurement systems such as optical measurement systems, laser trackers, 3-D stereoscopic cameras, and additional encoders have been used to determine the position of an end-effector accurately, thus facilitating the detection of deflections in the manipulators. Figure 12 shows the experimental setup for a robotic machining system equipped with a laser tracker for six-dimensional (6-D) pose measurements. Schneider et al. [108] proposed a fully closed position controller that uses an optical measurement system as a pose sensor. The offset between the intended and measured

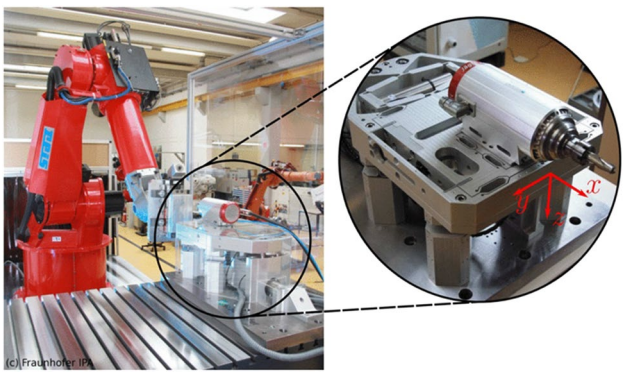

Fig. 11 Experimental setup of the robotic machining system including piezo-actuated high dynamic compensation system (HDCM) [104]. (Adapted from Ref. [104] with permission)

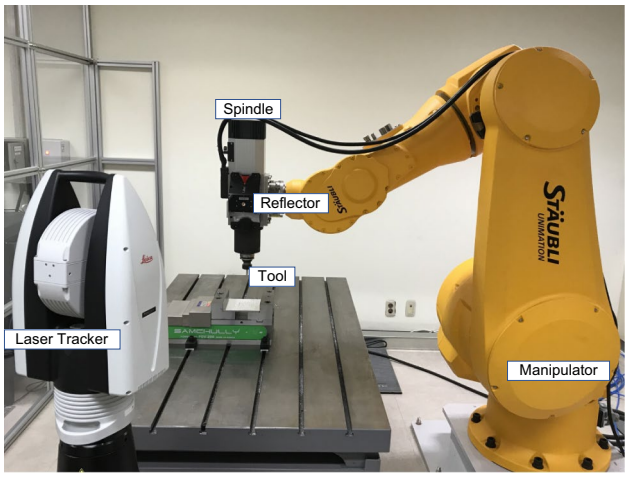

Fig. 12 Robotic machining system equipped with laser tracker

poses was calculated in Cartesian space and transformed into joint space using the inverse Jacobian. The sum of the calculated joint offset and the position command generated by the CNC was input to the servo drivers for each axis. In the experiments, the system was used to machine circles on steel workpieces. The experimental results confirmed that the pose accuracy of the end-effector improved significantly, reducing the machining error, expressed in terms of mean absolute error, from 253 to 63 μm.

Droll [109] introduced path correction for industrial robots using a laser tracker. Using a similar system configuration, Moeller et al. [110] employed a laser tracker to compare the position accuracy of factory standard, 3-D controlled, and 6-D controlled robots. In the case of the 6-D controlled configuration, the pose of the end-effector was measured using a 6-D probe. In the 3-D controlled configuration, the position of the end-effector was measured with a reflector. The 3-D system could not measure the orientation of the end-effector, thus inducing tool center point (TCP) error. Therefore, a reflector was attached close to the TCP to reduce the TCP error while controlling the robot in a 3-D configuration. Nevertheless, according to the comparison of the three configurations tested in the milling experiment, the path accuracy improved in the cases of the 3-D and 6-D controlled robots. The factory-standard configuration was observed to have a path error between 0.5 and 1.0 mm, while the path errors of the 3-D and 6-D controlled robots were less than 0.5 mm.

Another way of enhancing the accuracy of machining robots is to use a double encoder system. The backlash and compliance issues related to the joint gearbox mean that the motor encoder cannot represent the actual joint angles between the links. Therefore, a secondary encoder can be attached to the robot links to measure joint angles directly. Furthermore, the use of double encoders can decouple the

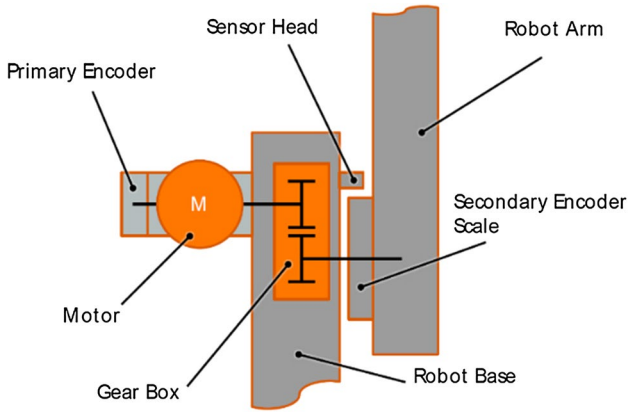

Fig. 13 Schematic diagram of double encoder system for robot manipulator [115]. (Adapted from Ref. [115] with permission)

deflection that occurs in the joint gearboxes and links. This makes it possible to use advanced stiffness models [111]. A commercial robot manufacturer has stated that vibration and overshooting can be controlled using the position output from a secondary encoder [112]. Robots with double encoder systems have been used to drill and mill aircraft parts in manufacturing field [113, 114].

Möller et al. [115] attached an inductive secondary encoder, as shown in Fig. 13, to a robot joint. An advanced control loop was applied, taking position outputs from both the motor encoder and the secondary encoder. Some features of commercial CNCs, such as friction compensation and torque pre-control, were also applied. In these experiments, robotic machining systems with double encoders were demonstrated to enhance bi-directional repeatability to 0.078 mm, while the repeatability of the system without a double encoder was 0.290 mm.

4.3 Mobile Platforms

Robotic machining systems have been equipped with additional stages to expand their workspaces [115, 116]. These additional stages enable such systems to machine large workpieces, such as aircraft wings. Manipulators have been installed on linear axis stages with a long stroke [113, 114], and on mobile platforms equipped with XYZ stages [117, 118] or wheels [119]. Fraunhofer IFAM proposed a mobile robotic system that consists of a mobile platform and a machining robot for large-scale CFRP parts, as shown in Fig. 14. One of the commercial mobile platforms is equipped with several Mecanum wheels, which enable the mobile machining system to move freely in the planar direction [120]. However, as the size of the workspace increases, it becomes more important to know the accurate relative pose of the robot base with respect to the workpiece. Therefore, Susemihl et al. [116] compared multiple referencing

Fig. 14 The mobile robot is processing the tail-fin of an Airbus 320 aircraft. (Courtesy of Fraunhofer IFAM)

strategies for mobile robotic systems. The multi-point best-fit strategy, which is also known as the point-cloud method, produced the best machining accuracy, with high robustness in repeated experiments, but the measurements required time and effort. The static helper-frame strategy required less effort but was only moderately robust and was less accurate.

5 Conclusion

In this review, robotic machining applications being adopted in industries have been summarized and recent research activities that improve the applicability of robotic machining systems have been reviewed. Various calibration methods for acquiring more accurate kinematic parameters of manipulators were also reviewed. To estimate and compensate compliance errors, sophisticated stiffness models and various compensation algorithms have been studied. Furthermore, auxiliary units used in robotic machining, that were installed to improve the performance of robotic machining system have been studied. Due to the efforts involved in improving robotic machining accuracy, application of robotic machining systems is expanding in automotive and aerospace industries where the size of workpiece is large. Shortly, robotic machining system will be gaining more attention for the replacement of machine tools in a variety of applications.

Acknowledgements This work was supported by the Technology Innovation Program (10053248, Development of Manufacturing System for Carbon Fiber Reinforced Plastics Machining) funded by the Ministry of Trade, Industry & Energy (MOTIE), Korea.

References

1. Chen, Y., & Dong, F. (2013). Robot machining: Recent development and future research issues. *International Journal of Advanced Manufacturing Technology, 66*(9–12), 1489–1497.

2. Chu, B., Kim, D., & Hong, D. (2008). Robotic automation technologies in construction: A review. *International Journal of Precision Engineering and Manufacturing, 9*(3), 85–91.
3. Pham, A.-D., & Ahn, H.-J. (2018). High precision reducers for industrial robots driving 4th industrial revolution: State of arts, analysis, design, performance evaluation and perspective. *International Journal of Precision Engineering and Manufacturing-Green Technology, 5*(4), 519–533.
4. Dieste, J. A., Fernández, A., Roba, D., Gonzalvo, B., & Lucas, P. (2013). Automatic grinding and polishing using spherical robot. *Procedia Engineering, 63,* 938–946.
5. Feng-yun, L., & Tian-sheng, L. (2005). Development of a robot system for complex surfaces polishing based on CL data. *International Journal of Advanced Manufacturing Technology, 26*(9), 1132–1137.
6. Tahvilian, A. M., Liu, Z., Champliaud, H., & Hazel, B. (2013). Experimental and finite element analysis of temperature and energy partition to the workpiece while grinding with a flexible robot. *Journal of Materials Processing Technology, 213*(12), 2292–2303.
7. Burghardt, A., Szybicki, D., Kurc, K., Muszyñska, M., & Mucha, J. (2017). Experimental study of Inconel 718 surface treatment by edge robotic deburring with force control. *Strength of Materials, 49*(4), 594–604.
8. Güvenç, L., & Srinivasan, K. (1997). An overview of robot-assisted die and mold polishing with emphasis on process modeling. *Journal of Manufacturing Systems, 16*(1), 48–58.
9. Dai, H., Yuen, K. M., & Elbestawi, M. A. (1993). Parametric modelling and control of the robotic grinding process. *International Journal of Advanced Manufacturing Technology, 8*(3), 182–192.
10. Haixia, Z., Shoucheng, W., Huiping, Z., Shanqing, L., & Shengxi, W. (2006). Research of polishing robot inverse calibration. In *Proceedings of world congress on intelligent control and automation* (pp. 2773–2776).
11. Huang, H., Gong, Z. M., Chen, X. Q., & Zhou, L. (2002). Robotic grinding and polishing for turbine-vane overhaul. *Journal of Materials Processing Technology, 127*(2), 140–145.
12. Ren, X., Kuhlenkötter, B., & Müller, H. (2006). Simulation and verification of belt grinding with industrial robots. *International Journal of Machine Tools and Manufacture, 46*(7), 708–716.
13. Liu, L., Ulrich, B., & Elbestawi, M. (1990). Robotic grinding force regulation: Design, implementation and benefits. In *Proceedings of IEEE international conference on robotics and automation* (pp. 258–265).
14. Whitney, D. (1985). Elements of an intelligent robot grinding system. In *Proceedings of the third ISRR* (pp. 381–387).
15. Takeuchi, Y., Ge, D., & Asakawa, N. (1993). Automated polishing process with a human-like dexterous robot. In *Proceedings of IEEE international conference on robotics and automation* (pp. 950–956).
16. Kunieda, M., & Nakagawa, T. (1985). Robot-polishing of curved surface with magneto-pressed tool and magnetic force sensor. In *Proceedings* of *the twenty-fifth international machine tool design and research conference* (pp. 193–200).
17. Xu, P., Li, B., Cheung, C.-F., & Zhang, J.-F. (2017). Stiffness modeling and optimization of a 3-DOF parallel robot in a serial–parallel polishing machine. *International Journal of Precision Engineering and Manufacturing, 18*(4), 497–507.
18. Norberto Pires, J., Ramming, J., Rauch, S., & Araújo, R. (2002). Force/torque sensing applied to industrial robotic deburring. *Sensor Review, 22*(3), 232–241.
19. Michalos, G., Makris, S., Papakostas, N., Mourtzis, D., & Chryssolouris, G. (2010). Automotive assembly technologies review: Challenges and outlook for a flexible and adaptive approach. *CIRP Journal of Manufacturing Science and Technology, 2*(2), 81–91.
20. Tung, P.-C., Wu, M.-C., & Hwang, Y.-R. (2004). An image-guided mobile robotic welding system for SMAW repair processes. *International Journal of Machine Tools and Manufacture, 44*(11), 1223–1233.
21. Wu, G., Wang, D., & Dong, H. (2017). Off-line programmed error compensation of an industrial robot in ship hull welding. In *Proceedings of intelligent robotics and applications* (pp. 135–146).
22. Tsoukantas, G., & Chryssolouris, G. (2008). Theoretical and experimental analysis of the remote welding process on thin, lap-joined AISI 304 sheets. *International Journal of Advanced Manufacturing Technology, 35*(9), 880–894.
23. Hu, Y., Kang, Y., Wang, X.-C., Li, X.-H., Long, X.-P., Zhai, G.-Y., et al. (2014). Mechanism and experimental investigation of ultra high pressure water jet on rubber cutting. *International Journal of Precision Engineering and Manufacturing, 15*(9), 1973–1978.
24. Lemma, E., Chen, L., Siores, E., & Wang, J. (2002). Study of cutting fiber-reinforced composites by using abrasive water-jet with cutting head oscillation. *Composite Structures, 57*(1), 297–303.
25. Biermann, D., Aßmuth, R., Schumann, S., Rieger, M., & Kuhlenkötter, B. (2016). Wet abrasive jet machining to prepare and design the cutting edge micro shape. *Procedia CIRP, 45,* 195–198.
26. Chen, D., Yuan, P., Wang, T., Cai, Y., & Xue, L. (2018). A compensation method for enhancing aviation drilling robot accuracy based on co-kriging. *International Journal of Precision Engineering and Manufacturing, 19*(8), 1133–1142.
27. Olsson, T., Haage, M., Kihlman, H., Johansson, R., Nilsson, K., Robertsson, A., et al. (2010). Cost-efficient drilling using industrial robots with high-bandwidth force feedback. *Robotics and Computer-Integrated Manufacturing, 26*(1), 24–38.
28. Olsson, T., Robertsson, A., & Johansson, R. (2007). Flexible force control for accurate low-cost robot drilling. In *Proceedings of IEEE international conference on robotics and automation* (pp. 4770–4775).
29. Lin, C.-T., & Wang, M.-J. (1999). Human–robot interaction in an aircraft wing drilling system. *International Journal of Industrial Ergonomics, 23*(1), 83–94.
30. Bu, Y., Liao, W., Tian, W., Zhang, L., & Dawei, L. I. (2017). Modeling and experimental investigation of Cartesian compliance characterization for drilling robot. *International Journal of Advanced Manufacturing Technology, 91*(9), 3253–3264.
31. Qin, C., Tao, J., Wang, M., & Liu, C. (2016). A Novel approach for the acquisition of vibration signals of the end effector in robotic drilling. In *Proceedings of IEEE international conference on aircraft utility systems* (pp. 522–526).
32. Bi, S., & Liang, J. (2011). Robotic drilling system for titanium structures. *International Journal of Advanced Manufacturing Technology, 54*(5), 767–774.
33. Gao, Y., Wu, D., Dong, Y., Ma, X., & Chen, K. (2017). The method of aiming towards the normal direction for robotic drilling. *International Journal of Precision Engineering and Manufacturing, 18*(6), 787–794.
34. Antunes Simões, J. F. C. P., Coole, T. J., Cheshire, D. G., & Pires, A. R. (2003). Analysis of multi-axis milling in an anthropomorphic robot, using the design of experiments methodology. *Journal of Materials Processing Technology, 135*(2), 235–241.
35. Slamani, M., Gauthier, S., & Chatelain, J.-F. (2014). Analysis of trajectory deviation during high speed robotic trimming of carbon-fiber reinforced polymers. *Robotics and Computer-Integrated Manufacturing, 30*(5), 546–555.

36. Cen, L., & Melkote, S. N. (2017). CCT-based mode coupling chatter avoidance in robotic milling. *Journal of Manufacturing Processes, 29,* 50–61.
37. Möller, C., Schmidt, H. C., Shah, N. H., & Wollnack, J. (2016). Enhanced absolute accuracy of an industrial milling robot using stereo camera system. *Procedia Technology, 26,* 389–398.
38. Matsuoka, S.-I., Shimizu, K., Yamazaki, N., & Oki, Y. (1999). High-speed end milling of an articulated robot and its characteristics. *Journal of Materials Processing Technology, 95*(1), 83–89.
39. Pan, Z., & Zhang, H. (2009). Improving robotic machining accuracy by real-time compensation. In *Proceedings of ICROS-SICE inter joint conference* (pp. 4289–4294).
40. Reinl, C., Friedmann, M., Bauer, J., Pischan, M., Abele, E., & Von Stryk, O. (2011). Model-based off-line compensation of path deviation for industrial robots in milling applications. In *Proceedings of IEEE/ASME international conference on advanced intelligent mechatronics* (pp. 367–372).
41. Abele, E., Weigold, M., & Rothenbücher, S. (2007). Modeling and identification of an industrial robot for machining applications. *CIRP Annals-Manufacturing Technology, 56*(1), 387–390.
42. Karan, B., & Vukobratovic, M. (1994). Calibration and accuracy of manipulation robot models—An overview. *Mechanism and Machine Theory, 29*(3), 479.
43. Elatta, A., Gen, L. P., Zhi, F. L., Daoyuan, Y., & Fei, L. (2004). An overview of robot calibration. *Information Technology Journal, 3*(1), 74–78.
44. Hwang, S., Kim, H., Choi, Y., Shin, K., & Han, C. (2017). Design optimization method for 7 DOF robot manipulator using performance indices. *International Journal of Precision Engineering and Manufacturing, 18*(3), 293–299.
45. Chen, X., Zhang, Q., & Sun, Y. (2019). Model-based compensation and Pareto-optimal trajectory modification method for robotic applications. *International Journal of Precision Engineering and Manufacturing*. https://doi.org/10.1007/s12541-019-00124-x.
46. Angelidis, A., & Vosniakos, G. C. (2014). Prediction and compensation of relative position error along industrial robot end-effector paths. *International Journal of Precision Engineering and Manufacturing, 15*(1), 63–73.
47. Liu, Z., Xu, J., Cheng, Q., Zhao, Y., Pei, Y., & Yang, C. (2018). Trajectory planning with minimum synthesis error for industrial robots using screw theory. *International Journal of Precision Engineering and Manufacturing, 19*(2), 183–193.
48. Meggiolaro, M. A., Dubowsky, S., & Mavroidis, C. (2005). Geometric and elastic error calibration of a high accuracy patient positioning system. *Mechanism and Machine Theory, 40*(4), 415–427.
49. Bogdan, I.-C., & Abba, G. (2009). identification of the servomechanism used for micro-displacement. In *Proceedings of IEEE/RSJ international conference on intelligent robots and systems*, pp. 1986–1991.
50. Gong, C., Yuan, J., & Ni, J. (2000). Nongeometric error identification and compensation for robotic system by inverse calibration. *International Journal of Machine Tools and Manufacture, 40*(14), 2119–2137.
51. Zhang, H., Wang, J., Zhang, G., Gan, Z., Pan, Z., Cui, H., et al. (2005). Machining with flexible manipulator: Toward improving robotic machining performance. In *Proceedings of IEEE/ASME international conference on advanced intelligent mechatronics* (pp. 1127–1132).
52. Marton, L., & Lantos, B. (2009). Friction and backlash measurement and identification method for robotic arms. In *Proceedings of international conference on advanced robotics* (pp. 1–6).
53. Barker, L. K. (1983). *Vector-algebra approach to extract Denavit–Hartenberg parameters of assembled robot arms*. NASA Technical Paper.
54. Hayati, S., & Mirmirani, M. (1985). Improving the absolute positioning accuracy of robot manipulators. *Journal of Robotic Systems, 2*(4), 397–413.
55. Ye, S. H., Wang, Y., Ren, Y. J., & Li, D. K. (2006). Robot calibration using iteration and differential kinematics. *Journal of Physics: Conference Series, 48,* 1–6.
56. Ha, I.-C. (2008). Kinematic parameter calibration method for industrial robot manipulator using the relative position. *Journal of Mechanical Science and Technology, 22*(6), 1084–1090.
57. Okamura, K., & Park, F. C. (1996). Kinematic calibration using the product of exponentials formula. *Robotica, 14*(4), 415–421.
58. Yang, X., Wu, L., Li, J., & Chen, K. (2014). A minimal kinematic model for serial robot calibration using POE formula. *Robotics and Computer-Integrated Manufacturing, 30*(3), 326–334.
59. Wu, L., Yang, X., Chen, K., & Ren, H. (2015). A minimal POE-based model for robotic kinematic calibration with only position measurements. *IEEE Transactions on Automation Science and Engineering, 12*(2), 758–763.
60. Cho, Y., Kim, M., Cheong, J., Do, H., & Kyung, J. (2017). Simultaneous identification of kinematic screw and joint compliance of elastic robot manipulators using deflected circular trajectories. In *Proceedings of IEEE/ASME international conference on advanced intelligent mechatronics* (pp. 382–387).
61. Zhou, J., Nguyen, H. N., & Kang, H. J. (2014). Simultaneous identification of joint compliance and kinematic parameters of industrial robots. *International Journal of Precision Engineering and Manufacturing, 15*(11), 2257–2264.
62. Jang, J. H., Kim, S. H., & Kwak, Y. K. (2001). Calibration of geometric and non-geometric errors of an industrial robot. *Robotica, 19*(3), 311–321.
63. Nubiola, A., & Bonev, I. A. (2013). Absolute calibration of an ABB IRB 1600 robot using a laser tracker. *Robotics and Computer-Integrated Manufacturing, 29*(1), 236–245.
64. Salisbury, J. K. (1980). Active stiffness control of a manipulator in Cartesian coordinates. In *Proceedings of IEEE conference on decision and control* (pp. 95–100).
65. Klimchik, A., Pashkevich, A., Wu, Y., Caro, S., & Furet, B. (2012). Design of calibration experiments for identification of manipulator elastostaticparameters. *Journal of Mechanics Engineering and Automation, 2*, 531–542.
66. Yoshikawa, T., & Matsudera, K. (1994). Experimental study on modeling of flexible manipulators using virtual joint model. *IFAC Proceedings Volumes, 27*(14), 427–432.
67. Caenen, J., & Angue, J. (1990). Identification of geometric and nongeometric parameters of robots. In *Proceedings of IEEE international conference on robotics and automation* (pp. 1032–1037).
68. Dumas, C., Caro, S., Cherif, M., Garnier, S., & Furet, B. (2012). Joint stiffness identification of industrial serial robots. *Robotica, 30*(4), 649–659.
69. Klimchik, A., Pashkevich, A., & Chablat, D. (2013). CAD-based approach for identification of elasto-static parameters of robotic manipulators. *Finite Elements in Analysis and Design, 75,* 19–30.
70. Corradini, C., Fauroux, J.-C., & Krut, S. (2003). Evaluation of a 4-degree of freedom parallel manipulator stiffness. In *Proceedings of world congress in mechanisms and machine science*.
71. Bouzgarrou, B., Fauroux, J., Gogu, G., & Heerah, Y. (2004). Rigidity analysis of T3R1 parallel robot with uncoupled kinematics. In *Proceedings of international symposium on robotics*.
72. Huang, T., Zhao, X., & Whitehouse, D. J. (2002). Stiffness estimation of a tripod-based parallel kinematic machine. *IEEE Transactions on Robotics and Automation, 18*(1), 50–58.
73. Clinton, C. M., Zhang, G., & Wavering, A. J. (1997). Stiffness modeling of a Stewart-platform-based milling machine. In *Transaction of the NorthAmerica manufacturing research institution of SME* (pp. 335–340).

74. Deblaise, D., Hernot, X., & Maurine, P. (2006). A systematic analytical method for PKM stiffness matrix calculation. In *Proceedings of IEEE international conference on robotics and automation* (pp. 4213–4219).
75. Gosselin, C. (1990). Stiffness mapping for parallel manipulators. *IEEE Transactions on Robotics and Automation, 6*(3), 377–382.
76. Chen, S.-F. (2003). The 6×6 stiffness formulation and transformation of serial manipulators via the CCT theory. In *Proceedings of IEEE international conference on robotics and automation* (pp. 4042–4047).
77. Chen, S.-F., & Kao, I. (2000). Conservative congruence transformation for joint and Cartesian stiffness matrices of robotic hands and fingers. *The International Journal of Robotics Research, 19*(9), 835–847.
78. Alici, G., & Shirinzadeh, B. (2005). Enhanced stiffness modeling, identification and characterization for robot manipulators. *IEEE Transactions on Robotics, 21*(4), 554–564.
79. Yoshikawa, T., & Hosoda, K. (1996). Modeling of flexible manipulators using virtual rigid links and passive joints. *The International Journal of Robotics Research, 15*(3), 290–299.
80. Abele, E., Rothenbücher, S., & Weigold, M. (2008). Cartesian compliance model for industrial robots using virtual joints. *Production Engineering, 2*(3), 339–343.
81. Schneider, U., Momeni-K, M., Ansaloni, M., & Verl, A. (2014). Stiffness modeling of industrial robots for deformation compensation in machining. In *Proceedings of IEEE/RSJ international conference on intelligent robots and systems* (pp. 4464–4469).
82. Marie, S., Courteille, E., & Maurine, P. (2013). Elasto-geometrical modeling and calibration of robot manipulators: Application to machining and forming applications. *Mechanism and Machine Theory, 69,* 13–43.
83. Lehmann, C., Olofsson, B., Nilsson, K., Halbauer, M., Haage, M., Robertsson, A., et al. (2013). Robot joint modeling and parameter identification using the clamping method. *IFAC Proceedings Volumes, 46*(9), 813–818.
84. Olabi, A., Damak, M., Bearee, R., Gibaru, O., & Leleu, S. (2012). Improving the accuracy of industrial robots by offline compensation of joints errors. In *Proceedings of IEEE international conference on industrial technology* (pp. 492–497).
85. Dumas, C., Caro, S., Garnier, S., & Furet, B. (2011). Joint stiffness identification of six-revolute industrial serial robots. *Robotics and Computer-Integrated Manufacturing, 27*(4), 881–888.
86. Klimchik, A., Ambiehl, A., Garnier, S., Furet, B., & Pashkevich, A. (2017). Efficiency evaluation of robots in machining applications using industrial performance measure. *Robotics and Computer-Integrated Manufacturing, 48,* 12–29.
87. Slavković, N. R., Milutinović, D. S., Kokotović, B. M., Glavonjić, M. M., Živanović, S. T., & Ehmann, K. F. (2013). Cartesian compliance identification and analysis of an articulated machining robot. *FME Transactions, 41*(2), 83–95.
88. Klimchik, A., Bondarenko, D., Pashkevich, A., Briot, S., & Furet, B. (2014). Compliance error compensation in robotic-based milling. In *Proceedings of informatics in control automation and robotics* (pp. 197–216).
89. Klimchik, A., Chablat, D., & Pashkevich, A. (2014). Stiffness modeling for perfect and non-perfect parallel manipulators under internal and external loadings. *Mechanism and Machine Theory, 79,* 1–28.
90. Klimchik, A., Wu, Y., Caro, S., Furet, B., & Pashkevich, A. (2014). Geometric and elastostatic calibration of robotic manipulator using partial pose measurements. *Advanced Robotics, 28*(21), 1419–1429.
91. Tyapin, I., Hovland, G., & Brogårdh, T. (2014). Method for estimating combined controller, joint and link stiffnesses of an industrial robot. In *Proceedings of IEEE international symposium on robotic and sensors environments* (pp. 1–6).
92. Cordes, M., & Hintze, W. (2017). Offline simulation of path deviation due to joint compliance and hysteresis for robot machining. *International Journal of Advanced Manufacturing Technology, 90*(1–4), 1075–1083.
93. Abele, E., Schützer, K., Bauer, J., & Pischan, M. (2012). Tool path adaption based on optical measurement data for milling with industrial robots. *Production Engineering, 6*(4–5), 459–465.
94. Tyapin, I., Kaldestad, K. B., & Hovland, G. (2015). Off-line path correction of robotic face milling using static tool force and robot stiffness. In Proceedings of *IEEE/RSJ international conference on intelligent robots and systems* (pp. 5506–5511).
95. Reiner, M., Otter, M., & Ulbrich, H. (2010). modeling and feedforward control of structural elastic robots. In *Proceedings of international conference on numerical analysis and applied mathematics* (pp. 378–381).
96. Roesch, O., & Zaeh, M. F. (2014). Fuzzy controller for the compensation of path deviations during robotic milling operations. In *Proceedings of IEEE international conference on mechatronics and automation* (pp. 192–197).
97. Wang, J., Zhang, H., & Fuhlbrigge, T. (2009). Improving machining accuracy with robot deformation compensation. In *Proceedings of IEEE/RSJ international conference on intelligent robots and systems* (pp. 3826–3831).
98. Zaeh, M. F., & Roesch, O. (2014). Improvement of the machining accuracy of milling robots. *Production Engineering, 8*(6), 737–744.
99. Lehmann, C., Halbauer, M., Euhus, D., & Overbeck, D. (2012). Milling with industrial robots: Strategies to reduce and compensate process force induced accuracy influences. In *Proceedings of IEEE 17th conference on emerging technologies & factory automation* (pp. 1–4).
100. Guo, Y., Dong, H., & Ke, Y. (2015). Stiffness-oriented posture optimization in robotic machining applications. *Robotics and Computer-Integrated Manufacturing, 35,* 69–76.
101. Bu, Y., Liao, W., Tian, W., Zhang, J., & Zhang, L. (2017). Stiffness analysis and optimization in robotic drilling application. *Precision Engineering, 49,* 388–400.
102. Lin, Y., Zhao, H., & Ding, H. (2017). Posture optimization methodology of 6R industrial robots for machining using performance evaluation indexes. *Robotics and Computer-Integrated Manufacturing, 48,* 59–72.
103. Lehmann, C., Pellicciari, M., Drust, M., & Gunnink, J. W. (2013). Machining with industrial robots: The COMET project approach. In *Proceedings of robotics in smart manufacturing* (pp. 27–36).
104. Sörnmo, O., Olofsson, B., Schneider, U., Robertsson, A., & Johansson, R. (2012). Increasing the milling accuracy for industrial robots using a piezo-actuated high-dynamic micro manipulator. In *Proceedings of IEEE/ASME international conference on advanced intelligent mechatronics* (pp. 104–110).
105. Puzik, A., Meyer, C., & Verl, A. (2010). Robot machining with additional 3-D-piezo-actuation-mechanism for error compensation. In Proceedings of *41st international symposium on robotics and 6th german conference on robotics* (pp. 1–7).
106. Schneider, U., Drust, M., Puzik, A., & Verl, A. (2013). Compensation of errors in robot machining with a parallel 3D-piezo compensation mechanism. *Procedia CIRP, 7,* 305–310.
107. Olofsson, B., Sörnmo, O., Schneider, U., Robertsson, A., Puzik, A., & Johansson, R. (2011). Modeling and control of a piezo-actuated high-dynamic compensation mechanism for industrial robots. In *Proceedings of IEEE/RSJ international conference on intelligent robots and systems* (pp. 4704–4709).
108. Schneider, U., Drust, M., Diaz Posada, J., & Verl, A. (2013). Position control of an industrial robot using an optical measurement system for machining purposes. In *Proceedings of international conference on manufacturing research* (pp. 307–312).

109. Droll, S. (2014). Real time path correction of industrial robots with direct end-effector feedback from a laser tracker. *SAE International Journal of Aerospace, 7*(2), 222–228.
110. Moeller, C., Schmidt, H. C., Koch, P., Boehlmann, C., Kothe, S., Wollnack, J., et al. (2017). Real time pose control of an industrial robotic system for machining of large scale components in aerospace industry using laser tracker system. *SAE International Journal of Aerospace, 10*(2), 100–108.
111. Klimchik, A., & Pashkevich, A. (2018). Robotic manipulators with double encoders: Accuracy improvement based on advanced stiffness modeling and intelligent control. *IFAC-PapersOnLine, 51*(11), 740–745.
112. Tsai, J., Wong, E., Tao, J., McGee, H. D., & Akeel, H. (2013). *Secondary position feedback control of a robot*. US8473103B2.
113. Saund, B., & DeVlieg, R. (2013). High accuracy articulated robots with CNC control systems. *SAE International Journal of Aerospace, 6*(2), 780–784.
114. Devlieg, R. (2011). High-accuracy robotic drilling/milling of 737 inboard flaps. *SAE International Journal of Aerospace, 4*(2), 1373–1379.
115. Möller, C., Schmidt, H. C., Koch, P., Böhlmann, C., Kothe, S.-M., Wollnack, J., et al. (2017). Machining of large scaled CFRP-parts with mobile CNC-based robotic system in aerospace industry. *Procedia Manufacturing, 14,* 17–29.
116. Susemihl, H., Brillinger, C., Stürmer, S. P., Hansen, S., Boehlmann, C., Kothe, S., et al. (2017). *Referencing strategies for high accuracy machining of large aircraft components with mobile robotic systems*. SAE Technical Papers, Part F129883, September, 2017.
117. Logemann, T. (2016). *Mobile Robot Assembly Cell (RACe) for drilling and fastening*. SAE Technical Papers, October, 2016.
118. Adams, G. (2014). *Next generation mobile robotic drilling and fastening systems*. SAE Technical Papers, September, 2014.
119. Susemihl, H., Moeller, C., Kothe, S., Schmidt, H. C., Shah, N., Brillinger, C., et al. (2016). High accuracy mobile robotic system for machining of large aircraft components. *SAE International Journal of Aerospace, 9*(2), 231–238.
120. KUKA. *Mobile robotics KMR Quantec*. Available, https://www.kuka.com/-/media/kuka-downloads/imported/9cb8e311bfd744b4b0eab25ca883f6d3/kmr-quantec-en.pdf. Accessed 12 June 2019.

Publisher's Note Springer Nature remains neutral with regard to jurisdictional claims in published maps and institutional affiliations.

Seong Hyeon Kim is a Ph.D. student in Mechanical Engineering at Yonsei University, Seoul, Korea. His research interests include computerized numerical control, precision motion control and robotics.

Eunseok Nam is a Senior Researcher with the IT Converged Process R&D Group, Korea Institute of Industrial Technology (KITECH). His research interests are precision machining, micromachining, hybrid machining, process control and optimization.

Tae In Ha is a Ph.D. student in Mechanical Engineering at Yonsei University, Seoul, Korea. His research interests include robotics and computerized numerical control.

Soon-Hong Hwang is a Ph.D. student in Mechanical Engineering at Yonsei University, Seoul, Korea. His research interests include computerized numerical control and precision motion control.

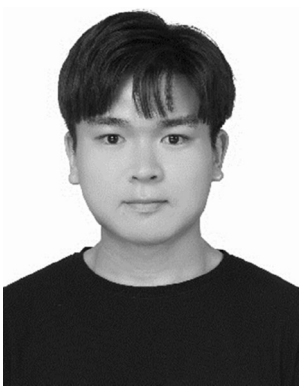

Jae Ho Lee is a Ph.D. student in Mechanical Engineering at Yonsei University, Seoul, Korea. His research interests include robotics and computerized numerical control.

Soo-Hyun Park is a Ph.D. student in Mechanical Engineering at Yonsei University, Seoul, Korea and Staff Engineer in the Global Technology Center, Samsung Electronics Co., Ltd. His research interest is virtual manufacturing, metal cutting, process planning, quantification of manufacturing process and simulation.

Byung-Kwon Min is a Professor with the Department of Mechanical Engineering, Yonsei University, Seoul, Korea. He received the B.S. and M.S. degrees from Yonsei University and the Ph.D. degree in mechanical engineering from University of Michigan. His research interests include machine tool control, precision manufacturing processes and intelligent manufacturing systems.